SLAC–PUB–5371
October 1990
T/E

NOVEL NUCLEAR AND HEAVY QUARK PHENOMENA IN QCD*

STANLEY J. BRODSKY

Stanford Linear Accelerator Center

Stanford University, Stanford, California 94309

ABSTRACT

A central focus of QCD studies is the non–perturbative structure of hadron wavefunctions, not only bound–state valence quark distributions, but also the intrinsic gluon and heavy quark distributions associated with higher Fock states. In this talk I discuss how the production of heavy quark systems and the use of nuclear targets can help to identify and separate the various components of hadron wavefunctions.

Invited talk presented at the QCD Workshop,
Montpellier, France, July 8-13, 1990

* Work supported by the Department of Energy, contract DE–AC03–76SF00515.

1. INTRODUCTION

Despite the elegant simplicity of its Lagrangian, the phenomenology of quantum chromodynamics is extraordinarily rich and complex. In this talk I will focus on QCD phenomena which reflect the coherence and composition of hadron wavefunctions as relativistic many–body systems of quark and gluon quanta. In the case of atomic physics, one can use external electromagnetic fields to modify atomic wavefunctions and to probe the underlying dynamics. Analogously, in QCD, we can study the dependence of reactions on the parameters of a nuclear medium to probe hadronic substructure and dynamics. In fact, we can use the nucleus as a differential "color filter" to separate Fock components (or fluctuations) of different transverse size in the projectile's wavefunction and to identify perturbative short–distance subprocesses versus non–perturbative mechanisms.

How can one define a wavefunction of a composite system in a relativistic quantum gauge field theory? A natural description, similar physically to that of the parton model, is to utilize a Fock expansion at fixed time $\tau = t - z/c$ on the light cone. This description is particularly simple since the perturbative vacuum is an apparent eigenstate of the full theory. As discussed at this conference by Werner,[1] the rigorous quantization of gauge theories on the light cone allows zero mode degrees of freedom of the gauge field in the vacuum sector which corresponds to non–zero chiral charge and other topological vacuum properties. In the particle sector of the theory, where one can quantize the theory in the light cone gauge $A^+ = 0$, one obtains a Fock basis containing only physical degrees of freedom.

The hadron eigenstate state can thus be expanded on the complete set of free quark and gluon eigenstates of the free QCD Hamiltonian which have the same

global quantum numbers as the hadron: *e.g.*:

$$
\begin{aligned}
|\Psi_p\rangle &= \sum |n\rangle \langle n \,|\, \Psi_p\rangle \\
&= |uud\rangle \, \psi_{uud}(x_i, k_{\perp i}, \lambda_i) \\
&\quad + |uudg\rangle \, \psi_{uudg}(x_i, k_{\perp i}, \lambda_i) \\
&\quad + |uudq\bar{q}\rangle \, \psi_{uudq\bar{q}}(x_i, k_{\perp i}, \lambda_i) \\
&\quad + \ldots
\end{aligned}
\tag{1}
$$

The x_i are the light–cone momentum fractions $x_i = (k^0 + k^z)/(P^0 + P^z)$, with $\sum_{i=1}^{n} x_i = 1$, and $\sum k_{\perp i} = 0$. The wavefunctions $\psi_n(x_1, k_{\perp i}, \lambda_i)$ appearing in the Fock–state expansion contain the physics of the hadron entering scattering amplitudes. For example, the structure functions measured in deep inelastic scattering are constructed as probability distributions in x from the sum of the squares of the light–cone wavefunctions $\psi_n(x_i, k_{\perp i}, \lambda_i)$. Similarly, since the current is a simple diagonal local operator on the free quark basis, form factors can be computed from a simple overlap integral of the ψ_n. More generally, high momentum transfer exclusive reactions in QCD are sensitive to the hadron distribution amplitudes $\phi(x_i, Q)$, which is the valence Fock amplitude integrated over transverse momentum up to the scale Q.

Recently, a new computational method, Discretized Light–Cone Quantization,[2] has been developed to compute the light–cone wavefunctions of hadrons. In this method one numerically diagonalizes the QCD Hamiltonian quantized on the light–cone in $A^+ = 0$ gauge. The basis is chosen as a complete set of discrete momentum–space color–singlet free gluon and quark Hamiltonian Fock states satisfying periodic and anti–periodic boundary conditions, respectively. In principle,

the eigenvalues of the full Hamiltonian provide the entire invariant mass spectrum, and the corresponding eigenfunctions provide the structure functions and distribution amplitudes needed for QCD factorization formulas. A major success of DLCQ has been applications to gauge theories in one–space and one–time dimensions.[2] For example, the complete spectrum and the respective structure functions of mesons, baryons, and nuclei in QCD(1+1) for $SU(3)_C$ have been obtained as a function of mass and coupling constant. Results for the structure function of the lowest mass meson and baryon at weak and strong coupling are shown in Fig. 1.

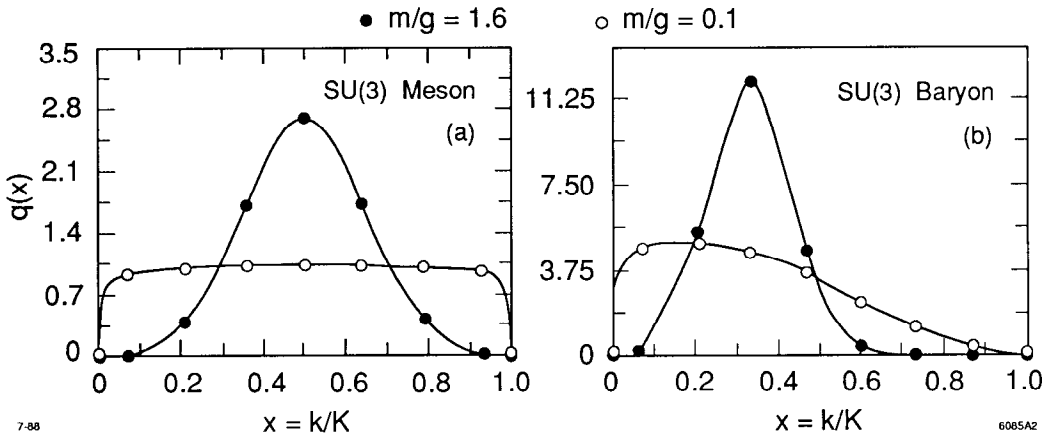

Figure 1. Valence structure functions of the baryon and meson in QCD in one–space and one–time dimension. The results are for one quark flavor and three colors.

The application of DLCQ to gauge theory in three–space and one–time dimensions is a much more challenging computational task, but progress has recently been made obtaining the spectrum of QED in the strong coupling domain.[3] The DLCQ formalism, including ultraviolet regularization, and Fock space truncation, is Lorentz–frame independent. Constraints on the non–perturbative structure of the proton in QCD models have also been obtained using bag models, quark–diquark schemes, QCD sum rules, non–relativistic quark models, and lattice gauge theory.

In this talk I will discuss a number of ways in which experiment can provide constraints on the light–cone Fock wavefunctions. It is necessary to distinguish "intrinsic" versus "extrinsic" contributions to scattering reactions. The intrinsic contributions, which are associated with multiparticle interactions within the hadron bound state, have lifetimes much longer than that of the time of collision; they are thus formed before the collision and lead to process–independent Feynman scaling production cross sections. Extrinsic contributions, on the other hand, are controlled by the high momentum transfer scale of the collision process itself and have short lifetimes of the same order as that of the collision time. For example, they provide the leading twist radiative corrections associated with the renormalization of single quark or gluon lines and lead to QCD evolution of structure functions.

An interesting new result, which I will discuss in Section 4, is that the valence distributions measured in deep inelastic lepton scattering are actually not identical to the bound state valence quark distributions because of a subtle effect due to Pauli blocking. I will also discuss in Section 3 some new results for the intrinsic polarized and unpolarized gluon distributions of the proton which are associated with hadron binding.

Because of asymptotic freedom, one can analyze short–distance, high momentum transfer, and heavy quark fluctuations of a hadronic wavefunction perturbatively.[4] The probability that a hadronic wavefunctions has far–off–shell fluctuations is only power–law suppressed in QCD because of the point–like character of the quark–gluon interactions. For example, the probability that a heavy quark pair exists virtually in a light hadron only decreases as $P_{Q\overline{Q}} \sim \alpha_s^2(M_Q^2)/M_Q^2$. Such intrinsic fluctuations have a Lorentz–boosted virtual lifetime of order $\tau \propto \gamma/M_Q^2$.

Thus they can be materialized in high energy collisions as projectile fragments. The dependence of the production cross section on the size of a nuclear target can be used as a filter to identify these intrinsic heavy quark processes. Further discussion is given in Section 5.

I also will discuss color transparency as a way to isolate strictly perturbative contributions to large angle exclusive scattering (see Section 2). In this analysis we will see how strong binding effects at the charm threshold can provides an interesting complication to perturbative QCD predictions. I also will discuss in Section 6 a new approach to shadowing and anti-shadowing of nuclear structure functions, and how these phenomena can provide information on the phase and magnitude of quark or gluon scattering amplitudes in the nuclear medium.

The above ingredients provide the foundations for analyzing many features of hadronic and heavy quark processes in high energy collisions including color transparency and intrinsic charm reactions.

2. The Nucleus as a QCD Filter

There are a large number of ways in which a nuclear target can probe fundamental aspects of QCD. A primary concept is that of the "color filter":[5,6] if the interactions of an incident hadron are controlled by gluon exchange, then the nucleus will be transparent to those fluctuations of the incident hadron wavefunction which have small transverse size. Such Fock components have a small color dipole moment and thus will interact weakly in the nucleus; conversely, Fock components of normal hadronic size will interact strongly and be absorbed during their passage through the nucleus.[5] For example, large momentum transfer quasi-exclusive reactions,[7] are controlled in perturbative QCD by small color-singlet valence-quark

Fock components of transverse size $b_\perp \sim 1/Q$; thus initial–state and final–state corrections to these hard reactions are suppressed at large momentum transfer, and they can occur in a nucleus without initial or final state absorption or multiple scattering of the interacting hadrons. Thus, at large momentum transfer and energies, quasi–elastic exclusive reactions are predicted to occur uniformly in the nuclear volume. This remarkable phenomenon is called "color transparency."[8] Thus QCD predicts that the transparency ratio of quasi–elastic annihilation of the anti–proton in the $\overline{p}p \to \ell\overline{\ell}$ reaction will be additive in proton number in a nuclear target:[9, 10]

$$\frac{\frac{d\sigma}{dQ^2}(\overline{p}A \to \ell\overline{\ell}(A-1))}{\frac{d\sigma}{dQ^2}(p\overline{p} \to \ell\overline{\ell})} \to Z^1 \tag{2}$$

for large pair–mass squared Q^2. In contrast to the QCD color transparency prediction, the traditional (Glauber) theory of nuclear absorption predicts that quasi–elastic scattering occurs primarily on the front surface of the nucleus. The above ratio thus should be proportional to $Z^{2/3}$, *i.e.* the number of protons exposed on the nuclear surface.

Conditions for Color Transparency — Color transparency is a striking prediction of perturbative QCD at high momentum transfers. There are two conditions which set the kinematic scale where the effect should be evident. First, the hard scattering subprocess must occur at a sufficiently large momentum transfer so that only small transverse size wavefunction components $\psi(x_i, b_\perp \sim 1/Q)$ with small color dipole moments dominate the reaction. Second, the state must remain small during its transit through the nucleus. The expansion distance is controlled by the time in which the small Fock component mixes with other Fock components. By Lorentz invariance, the time scale $\tau = 2E_{\overline{p}}/\Delta\mathcal{M}^2$ grows linearly with the energy of the hadron in the nuclear rest frame, where $\Delta\mathcal{M}^2$ is the difference of invariant

mass squared of the Fock components. Estimates for the expansion time are given in Refs. 6, 11, and 12.

There are a number of important tests of color transparency and color filter that can be carried out with anti-proton beams of moderate energy.[13] Since total annihilation processes such as $p\bar{p} \to \ell\bar{\ell}$ or $p\bar{p} \to \gamma\gamma$ and $p\bar{p} \to J/\psi$ automatically involve short distances, the first condition for color transparency should be satisfied. The study of the energy dependence of these processes inside nuclei (quasi-elastic reactions, integrated over Fermi-motion) can clarify the role of the expansion time scale τ. A recent analysis by Jennings and Miller[11] shows that $\tau = 2E_{\bar{p}}/\Delta\mathcal{M}^2$ is controlled by the mass difference of states which are close in mass to that of the asymptotic hadronic state. Thus color transparency may well be visible in low energy anti-proton annihilation processes, including quasi-elastic $\bar{p}p \to J/\psi$ and $\bar{p}p \to \bar{\ell}\ell$ annihilation in the nucleus.

The only existing test of color transparency is the measurement of quasi-elastic large angle pp scattering in nuclei at Brookhaven.[10] The transparency ratio is observed to increase as the momentum transfer increases, in agreement with the color transparency prediction. However, in contradiction to perturbative QCD expectations, the data suggests, surprisingly, that normal Glauber absorption seems to recur at the highest energies of the experiment $p_{\rm lab} \sim 12\ GeV/c$. It should be noted that this is the same kinematic domain where a strong spin correlation A_{NN} is observed.[14] The probability of protons scattering with their spins parallel and normal to the scattering plane is found to be twice that of anti-parallel scattering, which is again in strong contradiction to QCD expectations. However, Guy De Teramond and I[15] have noted that the breakdown of color transparency and the onset of strong spin-spin correlations can both be explained by the fact that the

charm threshold occurs in pp collisions at $\sqrt{s} \sim 5\ GeV$ or $p_{\rm lab} \sim 12\ GeV/c$. At this energy the charm quarks are produced at rest in the center of mass. Since all of the eight quarks have zero relative velocity, they can resonate to give a strong threshold effect in the $J = L = S = 1$ partial wave. (The orbital angular momentum of the pp state must be odd since the charm and anti–charm quarks have opposite parity.) This partial wave predicts maximal spin correlation in A_{NN}. Most important, such a threshold or resonant effect couples to hadrons of conventional size which will have normal absorption in the nucleus. If this non–perturbative $pp \to pp$ amplitude dominates over the perturbative QCD amplitude, one can explain both the large spin correlation and the breakdown of color transparency at the charm threshold. Thus the nucleus acts as a filter, absorbing the non–perturbative contribution to elastic pp scattering, while allowing the hard scattering perturbative QCD processes to occur additively throughout the nuclear volume.[16] Similarly, one expects that the charm threshold will modify the color transparency and hard–scattering behavior of quasi–elastic $\overline{p}p$ reactions in nuclei at energies $\sqrt{s} \sim 3\ GeV$.

Diffractive Production of Jets in Anti–Proton Nuclear Reactions — In our original paper on the color filter, Bertsch, Goldhaber, Gunion, and I[5] suggested that diffractive nuclear reactions could be used as a color filter, *i.e.* fluctuations of an incident hadron with small color dipole moments and hence could emerge unscathed after transit through a nucleus without nuclear excitation. In the case of anti–proton reactions, the fluctuations of the valence Fock state where the three anti–quarks has small transverse separation and thus small color dipole moment will be produced in the form of three jets on the back side of the nucleus. The longitudinal and transverse momentum dependence of the $\overline{p}A \to A\ Jet\ Jet\ Jet$ cross section will reflect the $\overline{qqq}$ composition of the incident anti–proton wavefunction.

The Color Filter and Hadron Fragmentation in Nuclei — Recently, Hoyer and I[17] have shown that the color filter ansatz can explain the empirical rule that the nuclear dependence of hadronic spectra $\frac{d\sigma/dx_F(HA\to H'X)}{d\sigma/dx_F(HN\to H'X)} = A^{\alpha(x_F)}$, is nearly independent of particle type H'. The essential point is that fluctuations of the initial hadron H which have the small transverse size have the least differential energy loss in the nucleus.

Color Transparency and Intrinsic Charm — A remarkable feature of the hadronic production of the J/ψ by protons in nuclei[18,19] is the fact that the cross section persists to high x_F, but with a strongly suppressed nuclear dependence, $A^{\alpha(x_F)} \sim 0.7$. The magnitude of the cross sections for high momentum charmonium reported by the NA–3 group[18] at CERN is, in fact, far in excess of what is predicted from gluon fusion or quark anti–quark annihilation subprocesses. Both the anomalous A–dependence and the high–x_F excess can be explained by assuming the presence of intrinsic charm components of the incident hadron wave–functions.[17] The essential physics point is as follows: the intrinsic charm Fock components, *e.g.* $|uudc\bar{c}\rangle$ in the proton have maximum probability when all of the quarks have equal velocities, *i.e.* when $x_i \propto \sqrt{m^2 + k_{\perp_i}^2}$. This implies that the charm and anti–charm quarks have the majority of the momentum of the proton when they are present in the hadron wavefunction. In a high energy proton–nucleus collision, the small transverse size, high–x intrinsic $c\bar{c}$ system can penetrate the nucleus, with minimal absorption and can coalesce to produce a charmonium state at large x_F. The remaining spectators of the nucleon tend to have more normal transverse size and interact on the front surface of the nucleus, leading to a production cross section approximately proportional to $A^{0.7}$. Since the formation of the charmonium state occurs far outside the nucleus at high energies, one predicts

similar $A^{\alpha(x_F)}$–dependence of the J/ψ and ψ' cross sections, in agreement with recent results reported by the E–772 experiment at Fermilab.[19] Further discussion on the implications of intrinsic charm is given in Section 5.

Shadowing, Anti–Shadowing of Inclusive Anti–Proton Reactions — In the case of inclusive reactions, such as Drell–Yan massive lepton pair production $p\bar{p} \to \ell\bar{\ell}X$, multiple scattering of the interacting partons in the nucleus can lead to shadowing and anti–shadowing of the nuclear structure functions and a shift of the pair's transverse momentum to large transverse momentum. Hung Jung Lu and I have shown that nuclear shadowing of leading–twist QCD reactions can be related to Pomeron exchange in the multiple interactions of the quark or anti–quark in the nucleus, and that the complex phase of the quark–nucleon scattering amplitude due to non–singlet Reggeon exchange leads to anti–shadowing; *i.e.* an excess of the nuclear cross section over nucleon additivity.[20] A detailed discussion will be given in Section 6.

Formation Zone Effects in Inclusive Reactions — An essential aspect of the proofs of QCD factorization of inclusive reactions such as Drell–Yan massive lepton pair production in a nuclear target is that the entire nuclear dependence of the cross section is contained in the nuclear structure functions as measured in deep inelastic lepton–nucleus scattering. Thus the factorization theorem predicts that there is no initial state absorption or scattering that can significantly modify an incident hadron's parton distributions as it propagates through the nucleus. In particular, induced hard colinear radiation due to inelastic reactions in the nucleus before the annihilation or hard–scattering subprocess occurs must be dynamically suppressed. As shown by Bodwin, Lepage, and myself,[21] this suppression occurs automatically in the nucleus due to the destructive interference of the various multiple–scattering

reactions in the nucleus. The interference occurs if the inelastic processes can occur coherently in the nucleus. This requires that the momentum transfer to target nucleons must be small compared to the inverse correlation length in the nucleus; *i.e.* $E_{\overline{q}} > \Delta\mathcal{M}^2 L_A > 1$, where E_q is the laboratory energy of the annihilating anti–quark, $\Delta\mathcal{M}^2$ is the change of mass squared of the quark in the inelastic reaction (small for hard colinear gluon emission of the anti–quark), and L_A is the length between target centers in the nucleus. This formation zone effect can be studied in detail by measuring the nuclear dependence as a function of anti–quark laboratory energy in anti–proton reactions.

Exclusive Nuclear Amplitudes — Exclusive nuclear reactions such as $\overline{p}d \to \gamma n$ or $\overline{p}d \to \pi^0 n$ can provide an important test of the reduced amplitude formalism for large momentum transfer exclusive nuclear reactions. Recent measurements at SLAC[22] are in striking agreement with the reduced amplitude predictions for photo–disintegration $\gamma d \to np$ at a surprising low momentum transfer. The corresponding anti–proton reactions will allow an important test of both the scaling behavior of exclusive nuclear reactions and their crossing behavior to the annihilation channel.

Hidden Color Nuclear Components — In QCD the six–quark deuteron is a linear superposition of five color singlet states, only one of which corresponds to the conventional $n - p$ state.[23] One can search for hidden color excitations of the deuteron in $\overline{p}He^3$ elastic scattering at large angles.

Nuclear Bound Quarkonium — The production of charmonium at threshold in a nuclear target is particularly interesting since it is possible that the attractive QCD van der Waals potential due to multi–gluon exchange could actually bind the η_c to light nuclei. Consider the reaction $\overline{p}\alpha \to (c\overline{c})H^3$ where the charmonium state

is produced nearly at rest. (See Fig. 2.) At the threshold for charm production, the incident nuclei will be nearly stopped (in the center of mass frame) and will fuse into a compound nucleus because of the strong attractive nuclear force. The charmonium state will be attracted to the nucleus by the QCD gluonic van der Waals force. One thus expects strong final state interactions near threshold. In fact, Guy De Teramond, Ivan Schmidt, and I[24] have argued that the $c\bar{c}$ system will bind to the H^3 nucleus. It is thus likely that a new type of exotic nuclear bound state will be formed: charmonium bound to nuclear matter. Such a state should be observable at a distinct $\bar{p}\alpha$ center of mass energy, spread by the width of the charmonium state, and it will decay to unique signatures such as $\bar{p}\alpha \rightarrow H^3\gamma\gamma$. The binding energy in the nucleus gives a measure of the charmonium's interactions with ordinary hadrons and nuclei; its hadronic decays will measure hadron–nucleus interactions and test color transparency starting from a unique initial state condition.

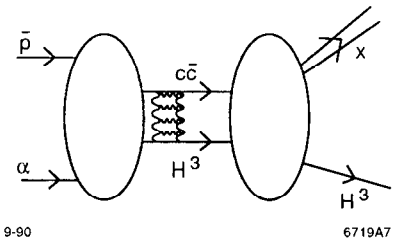

Figure 2. Formation of the $(c\bar{c}) - H^3$ bound state in the process $\bar{p}\alpha \rightarrow H^3X$.

In QCD, the nuclear forces are identified with the residual strong color interactions due to quark interchange and multiple–gluon exchange. Because of the identity of the quark constituents of nucleons, a short–range repulsive component is also present (Pauli–blocking). From this perspective, the study of heavy quarkonium interactions in nuclear matter is particularly interesting: due to the distinct

flavors of the quarks involved in the quarkonium–nucleon interaction there is no quark exchange to first order in elastic processes, and thus no one–meson–exchange potential from which to build a standard nuclear potential. For the same reason, there is no Pauli–blocking and consequently no short–range nuclear repulsion. The nuclear interaction in this case is purely gluonic and thus of a different nature from the usual nuclear forces.

The production of nuclear–bound quarkonium would be the first realization of hadronic nuclei with exotic components bound by a purely gluonic potential. Furthermore, the charmonium–nucleon interaction would provide the dynamical basis for understanding the spin–spin correlation anomaly in high energy $p - p$ elastic scattering.[15] In this case, the interaction is not strong enough to produce a bound state, but it can provide a strong enough enhancement at the heavy–quark threshold characteristic of an almost–bound system.[25]

3. The Intrinsic Gluon Distribution in of the Proton

The gluon distribution of a hadron is usually assumed to be radiatively generated from QCD evolution of the quark structure functions beginning at an initial scale Q_0^2.[26] In such a model one assumes that there are no gluons in the hadron at a resolution scale below Q_0. The evolution is completely incoherent; *i.e.* each quark in the hadron radiates independently.

However, as can be seen in the light–cone Hamiltonian approach, the higher Fock components of a bound state in QCD contain gluons at any resolution scale. The exchange of gluon quanta in the bound state generates an interaction potential; the retardation (energy–dependent) part of the potential contributes to the

intrinsic gluon distribution. Notice that the interference diagrams in which gluons are emitted from different quarks are not included in the usual extrinsic gluon distribution computed from the perturbative QCD evolution equations, since in leading twist these contributions only involve a single quark source.

The *intrinsic* gluon distribution $G_{g/H}(x, Q_0^2)$ describes the light–cone momentum distribution of gluons associated with the bound–state dynamics of the hadron H, in distinction to the *extrinsic* contributions which are derived from radiative processes or evolution from a single quark.

In the QCD case, the analysis of the intrinsic gluon distribution of a hadron is essentially non–perturbative. However, there are several theoretical constraints which limit its form:

1. In order to insure positivity of fragmentation functions, distribution functions $G_{a/b}(x)$ must behave as an odd or even power of $(1-x)$ at $x \to 1$ according to the relative statistics of a and b.[27] Thus the gluon distribution of a nucleon must have the behavior: $G_{g/N}(x) \sim (1-x)^{2k}$ at $x \to 1$ to ensure correct crossing to the fragmentation function $D_{N/g}(z)$. This result holds individually for each helicity of the gluon and the nucleon.

2. The coupling of quarks to gluons tends to match the sign of the quark helicity to the gluon helicity in the large x limit.[28] We define the helicity–aligned and anti–aligned gluon distributions: $G^+(x) = G_{g\uparrow/N\uparrow}(x)$ and $G^-(x) = G_{g\downarrow/N\uparrow}(x)$. The gauge theory couplings imply

$$\lim_{x\to 1} G^-(x)/G^+(x) \to (1-x)^2 \ . \tag{3}$$

3. In the low x domain, each of the quarks in the hadron radiate gluons coherently, and one must compute emission of gluons from the quark lines taking

into account interference between amplitudes. Define $\Delta G(x) = G^+(x) - G^-(x)$ and $G(x) = G^+(x) + G^-(x)$. We find that the asymmetry ratio $\Delta G(x)/G(x)$ vanishes linearly with x; perhaps coincidentally, this is also the prediction from Reggeon exchange.[29] The coefficient at $x \to 0$ depends on the hadronic wavefunctions; however, for equal partition of the hadron's momentum among its constituents, we show that

$$\lim_{x\to 0} \Delta G(x)/G(x) \to N_q \, x \ , \tag{4}$$

where N_q is the number of valence quarks.

4. In the $x \to 1$ limit, the stuck quark is far off–shell so that one can use perturbation theory to characterize the threshold dependence of the structure functions. We find for three–quark bound states

$$\lim_{x\to 1} G^+(x) \to C(1-x)^{2N_q-2} = C(1-x)^4 \ , \tag{5}$$

Thus $G^-(x) \to C(1-x)^6$ at $x \sim 1$. This is equivalent to the spectator–counting rule developed in Ref. 30.

We can write down a simple analytic model for the intrinsic gluon distribution in the nucleon which incorporates all of the above constraints:

$$\Delta G(x) = \frac{N}{x}[5(1-x)^4 - 4(1-x)^5 - (1-x)^6] \tag{6}$$

and

$$G(x) = \frac{N}{x}[5(1-x)^4 - 4(1-x)^5 + (1-x)^6] \tag{7}$$

In this model the momentum fraction carried by intrinsic gluons in the nucleon is $\langle x_g \rangle = \int_0^1 dx x G(x) = (10/21)N$, and the helicity carried by the intrinsic gluons is

$\Delta G \equiv \int_0^1 dx \Delta G(x) = 7/6N$. The ratio $\Delta G / \langle x_g \rangle = 49/20$ for the intrinsic gluon distribution is independent of the normalization N. Phenomenological analyses imply that the gluons carry approximately one–half of the proton's momentum: $\langle x_{g/N} \rangle \simeq 0.5$. We shall assume that this is a good characterization of the intrinsic gluon distribution. The momentum sum rule then implies $N \sim 1$ and $\Delta G \sim 1.2$. In terms of anomalous contributions to the quark spin is concerned, this is a relatively small contribution. However, since $\frac{1}{2} \sum \Delta q + \Delta G + L_z = \frac{1}{2}$, a large fraction of the proton's angular momentum is associated with the gluon distribution. A review of the present experimental and theoretical limits on gluon and quark spin in the nucleon is given in Ref. 31.

The above equations give model forms for the polarized and unpolarized intrinsic gluon distributions in the nucleon which take into account coherence at low x and perturbative constraints at high x. It is expected that this should be a good characterization of the gluon distribution at the resolution scale $Q_0^2 \simeq M_p^2$.

It is well–known that the leading power at $x \sim 1$ is increased when QCD evolution is taken into account. The change in power is

$$\Delta p_g(Q^2) = 4C_A \, \zeta(Q^2, Q_0^2) = \frac{1}{\pi} \int_{Q_0^2}^{Q^2} \frac{d\kappa^2}{\kappa^2} \alpha_s(\kappa^2) \, , \tag{8}$$

where $C_A = 3$ in QCD. For typical values of $Q_0 \sim 1 \; GeV$, $\Lambda_{\overline{MS}} \sim 0.2 \; GeV$ the change in power is moderate: $\Delta p_g(2 \; GeV^2) = 0.28$, $\Delta p_g(10 \; GeV^2) = 0.78$. A recent determination of the unpolarized gluon distribution of the proton at $Q^2 = 2 \; GeV^2$ using direct photon and deep inelastic data has been given in Ref. 32. The best fit over the interval $0.05 \leq x \leq 0.75$ assuming the form $xG(x, Q^2 = 2 \; GeV^2) = A(1-x)^{\eta_g}$ gives $\eta_g = 3.9 \pm 0.11 (+0.8 - 0.6)$, where the errors in parenthesis allow for

systematic uncertainties. This result is compatible with the prediction $\eta_g = 4$ for the intrinsic gluon distribution at the bound–state scale, allowing for the increase in the power due to evolution. HERA experiments could provide a definitive check on the shape and large–x behavior of the gluon structure function.

4. Bound Valence–Quark Distributions

An important concept in the description of any bound state is the definition of "valence" constituents. In atomic physics the term "valence electrons" refers to the electrons beyond the closed shells which give an atom its chemical properties. Correspondingly, the term "valence quarks" refers to the quarks which give the bound state hadron its global quantum numbers. In quantum field theory, the valence quarks appear in each Fock state together with any number of gluons and quark–anti–quark pairs; each component thus has the global quantum numbers of the hadron.

How can one identify the contribution of the valence quarks of the bound state with the phenomenological structure functions? Traditionally, the distribution function $G_{q/H}$ has been separated into "valence" and "sea" contributions:[33] $G_{q/H} = G^{\rm val}_{q/H} + G^{\rm sea}_{q/H}$, where, as an operational definition, one assumes

$$G^{\rm sea}_{q/H}(x,Q^2) = G^{\rm sea}_{\overline{q}/H}(x,Q^2), \qquad (0 < x < 1)\ , \tag{9}$$

and thus $G^{\rm val}_{q/H}(x,Q^2) = G_{q/H}(x,Q^2) - G_{\overline{q}/H}(x,Q^2)$. The assumption of identical quark and anti–quark sea distributions is plausible for the s and $\overline{s}$ quarks in the proton. However, in the case of the u and d quark contributions to the sea, anti–symmetrization of identical quarks in the higher Fock states implies non–identical

q and $\overline{q}$ sea contributions. This is immediately apparent in the case of atomic physics, where Bethe–Heitler pair production in the field of an atom does not give symmetric electron and positron distributions since electron capture is blocked in states where an atomic electron is already present. Similarly, in QCD, the $q\overline{q}$ pairs which arise from gluon splitting do not have identical quark and anti–quark sea distributions; contributions from interference diagrams, which arise from the anti–symmetrization of the higher Fock state wavefunctions, must be taken into account. Notice that because of wave–function normalization, the exclusion principle does not affect the value of conserved charges such as $\int_0^1 dx(G_{q/H}(x) - G_{\overline{q}/H}(x))$. Thus even though the conventional separation of valence and sea contributions gives correct charge sum rules,[34] it can give a misleading reading of the actual momentum distribution of the valence quarks. The standard definition also has the difficulty that the derived valence quark distributions are apparently singular in the limit $x \to 0$. For example, the expectation value of the light–cone kinetic energy operator

$$\int_0^1 dx \, \frac{\langle k_\perp^2 \rangle + m^2}{x} \, G_{q/p}(x, Q) \, . \tag{10}$$

is infinite for valence quarks if one uses the traditional definition. There is no apparent way of associating this divergence of the kinetic energy operator with renormalization.

Part of the difficulty with identifying bound state contributions to the proton structure functions is that many physical processes contribute to the deep inelastic lepton–proton cross section: From the perspective of the laboratory or center of mass frame, the virtual photon can scatter out a bound–state quark as in the atomic physics photoelectric process, or the photon can first make a $q\overline{q}$ pair, either

of which can interact in the target. As we emphasize here, in such pair–production processes, one must take into account the Pauli principle which forbids creation of a quark in the same state as one already present in the bound state wavefunction. Thus the lepton interacts with quarks which are both *intrinsic* to the proton's bound–state structure, and with quarks which are *extrinsic; i.e.* created in the electron–proton collision itself. Notice that such extrinsic processes would occur in electroproduction even if the valence quarks had no charge. Thus much of the phenomena observed in electroproduction at small values of x, such as Regge behavior, sea distributions associated with photon–gluon fusion processes, and shadowing in nuclear structure functions should be identified with the extrinsic interactions, rather than processes directly connected with the proton's bound–state structure.

Recently, Schmidt and I[35] have proposed a new definition of "bound valence–quark" distribution functions that correctly isolates the contribution of the valence constituents which give the hadron its flavor and other global quantum numbers. With this new separation, $G_{q/p}(x,Q^2) = G^{\rm BV}_{q/p}(x,Q^2) + G^{\rm NV}_{q/p}(x,Q^2)$, the non–valence quark distributions are identified with the structure functions which would be measured if the valence quarks of the target hadron had zero electro–weak charge. We can show that with this new definition the bound valence–quark distributions $G^{\rm BV}_{q/p}(x,Q^2)$ vanish at $x \to 0$, as expected from the wave function of a bound–state constituent.

In order to construct the bound valence–quark distributions, we imagine a *gedanken* QCD where, in addition to the usual set of quarks $\{q\} = \{u,d,s,c,b,t\}$, there is another set $\{q_0\} = \{u_0,d_0,s_0,c_0,b_0,t_0\}$ with the same spin, masses, flavor, color, and other quantum numbers, except that their electromagnetic charges are

zero. Let us now consider replacing the target proton p in the lepton–proton scattering experiment by a charge–less proton p_0 which has valence quarks q_0 of zero electromagnetic charge. In this extended QCD the higher Fock wavefunctions of the proton p and the charge–less proton p_0 both contain $q\overline{q}$ and $q_0\overline{q_0}$ pairs. As far as the strong QCD interactions are concerned, the physical proton and the *gedanken* charge–less proton are equivalent.

We then define (see Fig. 3) the bound valence–structure function of the proton from the difference between scattering on the physical proton minus the scattering on the charge–less proton, in analogy to an "empty target" subtraction:

$$F_i^{\rm BV}(x,Q^2) \equiv F_i^p(x,Q^2) - F_i^{p_0}(x,Q^2) \ . \tag{11}$$

The non–valence distribution is thus $F_i^{\rm NV}(x,Q^2) = F_i^{p_0}(x,Q^2)$. Here the $F_i(x,Q^2)$ ($i = 1,2$, etc.) are the leading twist structure functions. The situation just described is similar to the atomic physics case, where in order to correctly define photon scattering from a bound electron, one must subtract the cross section on the nucleus alone, without that bound electron present.[36] Physically, the nucleus can scatter photons through virtual pair production, and this contribution has to be subtracted from the total cross section. In QCD we cannot construct protons without the valence quarks; thus we need to consider hadrons with charge–less valence constituents.

Notice that pair production is not identical on the proton and null proton because of Pauli–blocking of identical quarks. In effect one subtracts a "capture" cross section where the quark is captured into the ground state. At high energies the capture and photo–absorption cross sections identically cancel since they are equal after charge conjugation and $s \leftrightarrow u$ crossing. (See Fig. 4.)

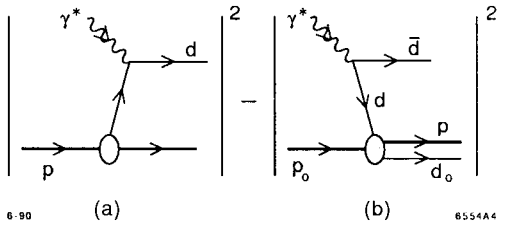

Figure 3. The bound valence–quark distribution of quark d is calculated from the difference between (a) the cross section on the state $p(uud)$ in which the virtual photon momentum is absorbed by the quark d, and (b) the $d\bar{d}$ pair production cross section in the field of the gedanken baryon $p_0(uud_0)$, where the produced d quark is captured in the same state as the d quark in the original proton state p.

If we write $s\sigma_{\rm photoelectric}$ as a sum of Regge terms of the form $\beta_R|s|^{\alpha_R}$, where $\alpha_R > 0$ then the subtraction of the capture cross section on the null proton will give the net virtual photo–absorption cross section as a difference of terms $s\sigma^{\rm BV} = \sum_R \beta_R(|s|^{\alpha_R} - |u|^{\alpha_R})$. If we ignore mass corrections in leading twist, then $s \simeq Q^2(1-x)/x$ and $u \simeq -Q^2/x$. Thus for small x every Regge term is multiplied by a factor $K_R = (-\alpha_R)x$. For example, for $\alpha_R = 1/2$ (which is the leading even charge–conjugation Reggeon contribution for non–singlet isospin structure functions), $F_2^{p(uud)} - F_2^{p_0(uud_0)} \sim x^{3/2}$. The bound valence–quark non–singlet ($I = 1$) distribution thus has leading behavior $G^{\rm BV}_{q/H} \sim x^{1/2}$ and vanishes for $x \to 0$. We can also understand this result from symmetry considerations. We have shown from crossing symmetry $G_{q/p}(x,Q^2) - G_{\bar{q}/p_0}(x,Q^2) \to 0$ at low x. Thus the even charge–conjugation Reggeon and Pomeron contributions decouple from the bound valence–quark distributions.

The essential reason why the new definition of the bound valence–quark distribution differs from the conventional definition of valence distributions is the Pauli principle: the anti–symmetrization of the bound state wavefunction for states which contain quarks of identical flavor. As we have shown, this effect plays a

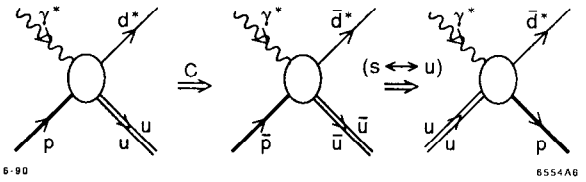

Figure 4. The helicity–summed squared amplitude for (a) $\gamma^* p \to d(uu)$ is equal, by charge conjugation, to the helicity–summed squared amplitude for the process (b) $\gamma^* \overline{p} \to \overline{d}(\overline{uu})$, up to a phase. This is also equal, by crossing symmetry, to the helicity–summed squared amplitude for (c) $\gamma^*(uu) \to \overline{d}p$, with s and u interchanged.

dynamical role at low x, eliminating leading Regge behavior in the bound valence–quark distributions. In the atomic physics case, where there is no leading Regge behavior, the analogous application of the Pauli principle leads to analytic consistency with the Kramers–Kronig dispersion relation for Compton scattering on a bound electron.[36]

5. Intrinsic Charm–Quark Distributions

There are a number of striking anomalies in the data[37] for charm production which cannot be readily explained by conventional leading twist $gg \to c\overline{c}$ or $q\overline{q} \to c\overline{c}$ fusion subprocesses.

1. The EMC data[38] for the charm structure function of the nucleon appears to be too high at large x_{Bj}.
2. The LEBC bubble chamber data[39] for charm production in pp collisions indicates an excess of D events at large x_F. The excess is not associated with $D's$ that contain the proton's valence quark.
3. The cross section measured by the WA–62 group[40] for $\Sigma^- N \to \Xi(csu)X$ is too large and flat at large x_F.
4. The NA–3 data[18] for J/ψ production in pion–nucleus and proton–nucleus

collisions can be represented as two components: a normal contribution in the central region which is almost additive in nuclear number that can be accounted for by $gg \to c\bar{c}$ and $q\bar{q} \to c\bar{c}$ fusion, and a second "diffractive contribution" which dominates at large x_F and is strongly shadowed. This last contribution suggests that high momentum $c\bar{c}$ systems are being produced on the front surface of the nuclear target.

It is difficult to understand any of these anomalies, particularly the production of high x_F charmonium unless the proton itself has an intrinsic charm contribution[41] to its structure function. From the perturbative point of view, a $uudc\bar{c}$ Fock component can be generated by the $gg \to c\bar{c}$ amplitude where the gluons are emitted from two of the valence quarks. The probability for finding the heavy quark pair of mass $M_{Q\overline{Q}}$ or greater is thus of order $\alpha_s^2(M^2_{Q\overline{Q}})/M^2_{Q\overline{Q}}$ (see the introduction). Intrinsic charm is thus a higher twist mechanism. The leading twist extrinsic charm contributions depend on the logarithm of the heavy quark mass. Since the intrinsic charm quarks are associated with the bound–state equation for the proton, then all the partons tend to have equal velocity. Unlike normal sea quarks generated by evolution, this implies that the heaviest constituents, the intrinsic charm quarks, will take a large fraction of the proton's momentum. In a hadronic collision the c and $\bar{c}$ can coalesce to produce a charmonium state with the majority of the proton's momentum.[42] The EMC charm structure function data requires a 0.3 % probability for the intrinsic charm Fock state in the nucleon.[38]

According to the hard scattering picture of QCD, production cross sections involving large momentum transfer should factorize and be approximately additive in the nucleon number, $d\sigma_A = A^\alpha(x_F, p_T)d\sigma_N$ with $\alpha \sim 1$, up to the small shadowing and anti–shadowing corrections seen in deep inelastic lepton–nucleus

scattering. (See Section 6.) In the Drell–Yan process, large mass muon pair production, $\alpha \simeq 1$ for all x_F is indeed observed.[43] However, several experiments on open charm production show[37] that $\alpha(x_F \geq 0.2) \simeq 0.7 \ldots 0.8$. For small x_F, an indirect analysis[39] comparing different measurements of the total charm production cross section indicates $\alpha(x_F \simeq 0) \simeq 1$.

The most detailed data on the nuclear dependence of charm production is available from the hadroproduction of J/ψ. Here a decrease of α from $\alpha(x_F \simeq 0) \simeq 1$ to $\alpha(x_F \simeq 0.8) \simeq 0.8$ has been seen by several groups.[44] The analysis of Badier, *et al.*[18] is particularly interesting. They noted that the production of J/ψ at large x_F (up to $x_F \simeq 0.8$) cannot be explained by the gluon and light quark fusion mechanisms of perturbative QCD, due to the anomalous $A-$dependence. However, their $\pi^- A \to J/\psi + X$ data was well reproduced if, in addition to hard QCD fusion (with $\alpha = 0.97$), they included a "diffractive" component of J/ψ production at high x_F with $\alpha = 0.77$. Using their measured A–dependence to extract the "diffractive" component, they found that (for a pion beam) that the J/ψ distribution peaks at $x_F \simeq 0.5$ and dominates the hard scattering A^1 component for $x \geq 0.6$. The anomalous nuclear dependence cannot be explained by gluon shadowing since the data scale in x_F rather than the gluon momentum fraction in the nucleus x_2.[45] Final state absorption of the charmonium state would predict an increasing nuclear yield with J/ψ momentum, opposite what is seen. Furthermore, this would not explain the similar $A-$dependence observed by E–772[19] for J/ψ and ψ' production.

A diffractive contribution to heavy quarkonium production is consistent with QCD when one takes into account the higher twist intrinsic charm component of the projectile wavefunction. In high energy hadron–nucleus collisions the nucleus

may be regarded as a "filter" of the hadronic wave function.[5] The argument, which relies only on general features such as time dilation, goes as follows.[46] As discussed in the introduction, one can define a Fock state expansion of a hadron in terms of its quark and gluon constituents; *e.g.* for a meson,

$$|h\rangle = |q\bar{q}\rangle + |q\bar{q}g\rangle + |q\bar{q}q\bar{q}\rangle + \ldots \tag{12}$$

The various Fock components will mix with each other during their time evolution. However, at sufficiently high hadron energies E_h, and during short times t, the mixing is negligible. Specifically, the relative phase $\exp[-i(E - E_h)t]$ of a given term in Eq. (1) is proportional to the energy difference

$$E - E_h = \left[\sum_i \frac{m_i^2 + \mathbf{p}_{Ti}^2}{x_i} - M_h^2\right] \Big/ (2E_h) \tag{13}$$

which vanishes for $E_h \to \infty$. Hence the time evolution of the Fock expansion is, at high energies, diagonal during the time $\sim 1/R$ it takes for the hadron to cross a nucleus of radius R.

The diagonal time development means that it is possible to describe the scattering of a hadron in a nucleus in terms of the scattering of its individual Fock components. Let us explore the consequences for typical, soft collisions characterized by momentum transfers $q_T \simeq \Lambda_{QCD}$. The partons of a given Fock state will scatter independently of each other if their transverse separation is $r_T \geq 1/\Lambda_{QCD}$; *i.e.* if the state is of typical hadronic size. Conversely, the nuclear scattering will be coherent over the partons in Fock states having $r_T \ll 1/\Lambda_{QCD}$ since $e^{i\mathbf{q}_T \cdot \mathbf{r}_T} \simeq 1$. For color–singlet clusters, the interference between the different parton amplitudes interacting with the nuclear gluonic field is destructive. Thus the nucleus will

appear nearly transparent to small, color–singlet Fock states. In an experiment detecting fast secondary hadrons the nucleus indeed serves, then, as a filter that selects the small Fock components in the incident hadrons.

Now consider the intrinsic charm state $|u\bar{d}c\bar{c}\rangle$ of a $|\pi^+\rangle$. Because of the large charm mass m_c, the energy difference in denominator of the wavefunction will be minimized at equal parton velocity; i.e., when the charm quarks carry most of the longitudinal momentum. Moreover, because m_c is large, the transverse momenta p_{Tc} of the charm quarks range up to $\mathcal{O}(m_c)$, implying that the transverse size of the $c\bar{c}$ system is $\mathcal{O}(1/m_c)$. Hence, provided only that the $c\bar{c}$ forms a color singlet, it can penetrate the nucleus with little energy loss. Thus the high momentum small transverse size $c\bar{c}$ color–singlet cluster in the incident hadron passes through the nucleus undeflected, and it can then evolve into charmonium states after transiting the nucleus.[47] In effect, the nucleus is transparent to the heavy quark pair component of the intrinsic state. The remaining cluster of light quarks in the intrinsic charm Fock state ranging in transverse size up to the typical hadronic scale and tends to be absorbed on the front surface of the nucleus. This justifies the analysis of Badier *et al.*in which the perturbative and non–perturbative charm production mechanisms were separated on the basis of their different A–dependence ($\alpha = 0.97$ and $\alpha = 0.77$ for a pion beam, respectively). The effective x_F–dependence of α seen in charm production is explained by the different characteristics of the two production mechanisms. Hard, gluon fusion production dominates at small x_F, due to the steeply falling gluon structure function. The contribution from intrinsic charm Fock states in the beam peaks at higher x_F, due to the large momentum carried by the charm quarks. This two–component hard–scattering plus intrinsic charm model also explains why the nuclear dependence of J/ψ production depends

on x_F rather than x_2, as predicted by leading twist factorization.[45]

An important consequence of this picture is that all final states produced by a penetrating intrinsic $c\bar{c}$ component will have the same A–dependence. Thus, in particular, the $\psi(2S)$ radially excited state will behave in the same way as the J/ψ, in spite of its larger size. This prediction is confirmed by the recent E–772 data.[19] The nucleus cannot influence the quark hadronization which (at high energies) takes place outside the nuclear environment.

Quarkonium production due to the intrinsic heavy quark state will fall off rapidly for p_T greater than M_Q, reflecting the fast–falling transverse momentum dependence of the higher Fock state wavefunction. Thus we expect the conventional fusion contributions to dominate in the large p_T region. The data are in fact consistent with a simple A^1 law for J/ψ production at large p_T. The CERN experiment of Badier *et al.*[18] finds that the ratio of nuclear cross sections is close to additive in A for all x_F when p_T is between 2 and 3 GeV. The data of the FermiLab experiment of Katsanevas *et al.*[44] shows consistency with additivity for p_T ranging from 1.2 to 3 GeV.

As was discussed above, the probability for intrinsic heavy quark states in a light hadron wave function is expected[41,48] to scale up to logarithms inversely as the square of the heavy quark mass. This implies a production cross section proportional to $1/M_Q^4$. The total rate of heavy quark production by the intrinsic mechanism therefore decreases with quark mass relative to the leading–twist cross section which is proportional to $1/M_Q^2$. At large x the intrinsic production should still dominate, however, implying a nuclear dependence in this region characterized by $\alpha \simeq 0.7 \ldots 0.8$. The recent E–772 data[19] for the hadroproduction of the upsilon suggests that intrinsic beauty contributions may also be playing a role.

Experimental measurements of beauty hadroproduction in nuclei over the whole range of x will be essential for unraveling the two components of the cross section.

6. Shadowing and Anti–Shadowing of Nuclear Structure Functions

The shadowing and anti–shadowing of deep inelastic nuclear structure functions refers to the depletion of the effective number of nucleons F_2^A/F_2^N at low $x \lesssim 0.1$, and the increase above nucleon additivity at $x \sim 0.15$. Results from the EMC collaboration[49] and SLAC[50] indicate that the effect is roughly Q^2–independent; *i.e.* shadowing is a leading twist in the operator product analysis. In contrast, the shadowing of the real photo–absorption cross section due to ρ–dominance[51–54] falls away as an inverse power of Q^2.

Shadowing is a destructive interference effect which causes a diminished flux and interactions in the interior and back face of the nucleus. The Glauber analysis[55] corresponds of hadron–nucleus scattering to the following: the incident hadron scatters elastically on a nucleon N_1 on the front face of the nucleus. At high energies the phase of the amplitude is imaginary. The hadron then propagates through the nucleus to nucleon N_2 where it interacts inelastically. The accumulated phase of the hadron propagator is also imaginary, so that this two–step amplitude is coherent and opposite in phase to the one–step amplitude where the beam hadron interacts directly on N_2 without initial–state interactions. Thus the target nucleon N_2 sees less incoming flux: it is shadowed by elastic interactions on the front face of the nucleus. If the hadron–nucleon cross section is large, then for large A the effective number of nucleons participating in the inelastic interactions is reduced to $\sim A^{2/3}$, the number of surface nucleons.

In the case of virtual photo–absorption, the photon converts to a $q\overline{q}$ pair at a distance before the target proportional to $\omega = x^{-1} = 2p \cdot q/Q^2$ in the laboratory frame.[56] In a physical gauge, such as the light–cone $A^+ = 0$ gauge, the final–state interactions of the quark can be neglected in the Bjorken limit, and effectively only the anti–quark interacts. The nuclear structure function F_2^A producing quark q can then be written as an integral[57,58] over the inelastic cross section $\sigma_{\overline{q}A}(s')$ where s' grows as $1/x$ for fixed space–like anti–quark mass. Similarly, the anti–quark nuclear structure function is related to inelastic quark–nucleus scattering. Thus the A–dependence of the deep inelastic nuclear structure functions cross section reflects the A–dependence of the q and $\overline{q}$ cross sections in the nucleus. Hung Jung Lu and I have recently applied the standard Glauber multi–scattering theory, to $\sigma_{\overline{q}A}$ and σ_{qA} assuming that formalism can be taken over to off–shell interactions.[59] The shadowing mechanism is illustrated in Fig. 5.

The predictions for the effective number of nucleons $A_{eff}(x)/A$ are shown in Fig. 6 for $A = 12$, 64, and 238. One observes shadowing below $x \simeq 0.1$ and an anti–shadowing peak around $x \simeq 0.15$. The shadowing effects are roughly logarithmic on the mass number A. The magnitude of shadowing predicted by the model is consistent with the data for $x > 0.01$; below this region, one expects higher–twist and vector–meson dominance shadowing to contribute. For $x > 0.2$ other nuclear effects must be taken into account. Most of the parameters used in the model are assigned typical hadronic values. The critical quantity is the effective quark–nucleon cross section σ which controls the magnitude of shadowing effect near $x = 0$: a larger value of σ implies a larger $\overline{q}^* N$ cross section and thus more shadowing. Notice that σ is the effective cross section at zero $\overline{q}$ virtuality, thus the typical value $\langle\sigma\rangle$ entering the calculation is somewhat smaller. The magnitude

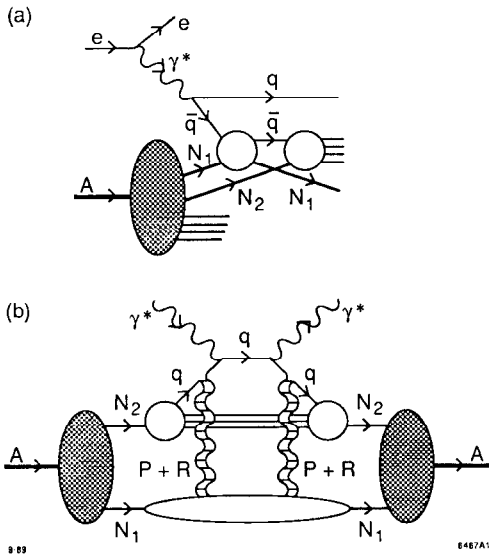

Figure 5. (a) The double–scattering amplitude that shadows the direct interaction of the anti–quark with N_2.
(b) The same mechanism as in (a), drawn in the traditional "hand–bag" form. Pomeron and Reggeon exchange between the quark line and N_1 are explicitly illustrated.

of anti–shadowing is determined the real–to–imaginary–part ratio of the Reggeon scattering amplitude.

Our semi–quantitative analysis shows that parton multiple–scattering process provides a mechanism for explaining the observed shadowing at low x in the EMC–SLAC data. The existence of anti–shadowing requires the presence of regions where the real part of the $\overline{q} - N$ amplitude dominates over the imaginary part. The constructive interference which gives anti–shadowing in the $x \sim 0.15$ region is due in this model to the phase of the Reggeon $\alpha = 1/2$ term. The phase follows from analyticity and is dictated by the shape of the structure functions at low x. We could utilize additional terms (at lower values of α) to parameterize other bound–state contributions which vanish as higher powers of x, but in practice their

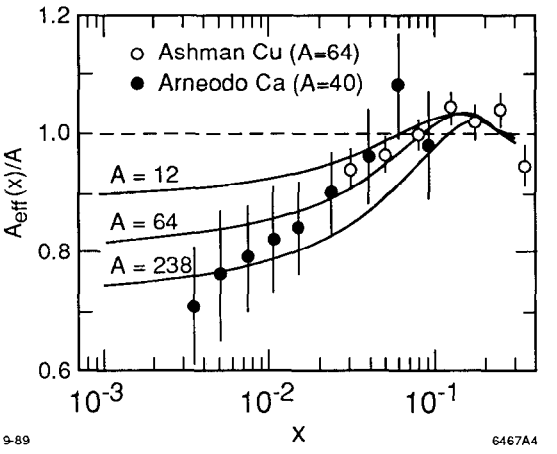

Figure 6. The predicted ratio of $A_{eff}(x)/A$ of the multi–scattering model in the low x region for different nuclear mass number. The data points are results from the EMC experiment for Cu and Ca.

qualitative effect would be indistinguishable from the our simplified model. These results show that for reasonable values of the quark– and anti–quark–nucleon cross section, one can understand the magnitude of the shadowing effect at small x. Moreover, if one introduces an $\alpha_R \simeq 1/2$ Reggeon contribution to the $\overline{q}N$ and qN amplitudes , the real phase introduced by such a contribution automatically leads to "anti–shadowing" (effective number of nucleons $F_2^A(x,Q^2)/F_2^N(x,Q^2) > A$) at $x \simeq 0.15$ of the few percent magnitude seen by the SLAC and EMC experiments.[49,50] The analysis also provides the input or starting point for the log Q^2 evolution of the deep inelastic structure functions, as given for example by Mueller and Qiu.[60] The parameters for the effective $\overline{q}$–nucleon cross section required to understand shadowing phenomena provide important information on the interactions of quarks in nuclear matter.

The analysis presented here correlates shadowing phenomena to microscopic quark–nucleon parameters. This approach also provides a dynamical and analytic explanation of anti–shadowing, confirming the conjecture of Nikolaev and

Zakharov[61] who predicted that such an effect must exist on the basis of conservation laws. Using the perturbative QCD factorization theorem for inclusive reactions, the same analysis can be extended to Drell–Yan and other fusion processes, taking into account the separate dependence on the valence and sea quarks. Thus some shadowing and anti–shadowing should also be observable in the nuclear structure function $F_2^A(x_2, Q^2)$ extracted from massive lepton pair production on nuclear targets at low x_2. However, unlike pion excess models, the non–additive nuclear effect is not restricted to sea quarks.

This microscopic approach to shadowing and anti–shadowing analysis also has implications of the nature of particle production for virtual photo–absorption in nuclei. At high Q^2 and $x > 0.3$, hadron production should be uniform throughout the nucleus. At low x where shadowing occurs, the inelastic reaction occurs mainly at the front surface. These features can be examined in detail by studying non–additive multi–particle correlations in both the target and current fragmentation region. The same types of multi–scattering "fan" diagrams also appear in the analysis of the saturation of the gluon distribution at small x.[62]

ACKNOWLEDGEMENTS

Some of the material presented here is based on collaborations with others, particularly G. de Teramond, J. R. Hiller, P. Hoyer, G. P. Lepage, H. J. Lu, A. H. Mueller, and I. Schmidt. I also wish to thank Stefan Narison and his colleagues at the University of Montpelier for their outstanding hospitality and a very interesting conference.

REFERENCES

1. E. Werner, this conference, and T. Heinzl, S. Krusche, E. Werner, Regensburg University preprint TPR–90–44 (1990).

2. K. Hornbostel, S. J. Brodsky, and H.–C. Pauli, Phys. Rev. D41, 3814 (1990); K. Hornbostel, SLAC–0333, Ph. D. thesis, unpublished (1988); and M. Burkardt, Nucl. Phys. A504, 762 (1989); and references therein.

3. A. Tang, S. Brodsky, H. C. Pauli, and M. Krautgartner, to be published.

4. S. J. Brodsky and P. Hoyer, to be published.

5. G. Bertsch, S. J. Brodsky, A. S. Goldhaber, and J. Gunion, Phys. Rev. Lett. 47, 297 (1981).

6. J. P. Ralston and B. Pire, Phys. Rev. Lett. 61, 1823 (1988), University of Kansas preprint 90–0548 (1990).

7. Exclusive processes in QCD are reviewed in S. J. Brodsky and G. P. Lepage, in *Quantum Chromodynamics*, edited by A.. H. Mueller, (World Scientific, 1990.)

8. A. H. Mueller, *Proc. XVII Recontre de Moriond* (1982); S. J. Brodsky, *Proc. XIII International Symposium on Multiparticle Dynamics*, Volendam (1982); S. J. Brodsky and A. H. Mueller, Phys. Lett. 206B, 685 (1988). and references therein.

9. By definition, quasi–elastic processes are nearly coplanar, integrated over the Fermi motion of the protons in the nucleus. Such processes are nearly exclusive in the sense that no extra hadrons are allowed in the final state.

10. A. S. Carroll, *et al.*, Phys. Rev. Lett. 61, 1698 (1988).

11. B. K. Jennings and G. A. Miller, Phys. Lett. B236, 209 (1990). and University of Washington preprint (1990).

12. G. R. Farrar, H. Liu, L. L. Frankfurt, M. I. Strikman, Phys. Rev. Lett. 61, 686 (1988).

13. For additional discussion, see also, A. B. Kaidalov, presented at the LEAR Workshop (1990).

14. G. R. Court, *et al.*, Phys. Rev. Lett. 57, 507 (1986).

15. S. J. Brodsky and G. de Teramond, Phys. Rev. Lett. 60, 1924 (1988).

16. For an alternative explanation, see Ref. 6.

17. S. J. Brodsky and P. Hoyer, Phys. Rev. Lett. 63, 1566 (1990); S. J. Brodsky, C. Peterson. and N. Sakai, Phys. Rev. D23, 2745 (1981). E. Hoffmann and R. Moore, Z. Phys. C20, 91 (1990). For a recent estimate of intrinsic charm matrix elements from OZI–violation in baryons, see T. Hatsuda and T. Kunihiro, CERN–TH. 5386 (1990).

18. J. Badier, *et al.*, Z. Phys. C20, 101 (1983); Phys. Lett. 104B, 335 (1981). P. Charpentier, Saclay Thesis CEA–N–237 (1984).

19. D. M. Alde, *et al.*, Phys. Rev. Lett. 64, 2479 (1990), Los Alamos preprint LA–UR–90–2331 (1990), and references therein.

20. S. J. Brodsky and H. J. Lu, Phys. Rev. Lett. 64, 1342 (1990).

21. G. T. Bodwin, S. J. Brodsky, and G. P. Lepage, Phys. Rev. D39, 3287 (1989).

22. J. Napolitano *et al.*, Phys. Rev. Lett. 61, 2530 (1988).

23. For a recent review on the status of di–baryon hidden color resonances, see E. Lomon, MIT preprint (1990).

24. S. J. Brodsky, G. de Teramond, and I. Schmidt, Phys. Rev. Lett. 64, 1011 (1990).

25. The signal for the production of almost–bound nucleon (or nuclear) charmonium systems near threshold is the isotropic production of the recoil nucleon (or nucleus) at large invariant mass $M_X \simeq M_{\eta_c}$.

26. See, e. g., F. Martin, Phys. Rev. D19, 1382 (1979); M. Glück, E. Reya, and W. Vogelsang, Dortmund University preprint DO–TH–89/3 (1989).

27. V. N. Gribov and L. N. Lipatov, Sov. J. Nucl. Phys. 15, 438 and 675 (1972).

28. J. D. Bjorken, Phys. Rev. D1, 1376 (1970).

29. See, for example, S. J. Brodsky, J. Ellis, M. Karliner, Phys. Lett. B206, 309 (1988).

30. R. Blankenbecler, S. J. Brodsky Phys. Rev. D10, 2973 (1974); J. F. Gunion, Phys. Rev. D10, 242 (1974); S. J. Brodsky and J. F. Gunion, Phys. Rev. D19, 1005 (1979).

31. M. Karliner, 24th Rencontre de Moriond, Mar 1989; preprint TAUP 1730–89.

32. P. Aurenche, *et al.*, Phys. Rev. D39, 3275 (1989).

33. See, for example, F. E. Close, *An Introduction to Quarks and Partons*, Academic Press (1979).

34. It is interesting to notice that the Gottfried sum rule assumes the equality of anti–up and anti–down quarks in the proton. Because of the stronger Pauli blocking of up quarks, however, one would expect a relative suppression of anti–up quarks in the proton, giving a correction to the sum rule.

35. S. J. Brodsky and I. A. Schmidt, SLAC–PUB–5169 (1990), to be published in Phys. Rev. D.

36. M. L. Goldberger and F. E. Low, Phys. Rev. 176, 1778 (1968); see also: T. Erber, Ann. Phys. 6, 319 (1959).

37. S. P. K. Tavernier, Rep. Prog. Phys. 50, 1439 (1987); U. Gasparini, *Proc. XXIV Int. Conf. on High Energy Physics*, (R. Kotthaus and J. H. Kühn, Eds., Springer 1989), p. 971.

38. Detailed predictions for the contribution of intrinsic charm to the nucleon charmed quark structure functions and comparisons with existing lepto–production data are given by E. Hoffmann and R. Moore, Ref. 17.

39. M. MacDermott and S. Reucroft, Phys. Lett. 184B, 108 (1987).

40. S. F. Biagi, *et al.*, Z. Phys. C28, 175 (1985). See also P. Coteus, *et al.*. Phys. Rev. Lett. 59, 5030 (1987).

41. S. J. Brodsky, P. Hoyer, C. Peterson, and N. Sakai, Phys. Lett. 93B, 451 (1980); S. J. Brodsky, C. Peterson, and N. Sakai, Phys. Rev. D23, 2745 (1981).

42. S. J. Brodsky, J. F. Gunion, and D. E. Soper, Phys. Rev. D36, 2710 (1987).

43. K. J. Anderson, *et al.*, Phys. Rev. Lett. 42, 944 (1979); A. S. Ito, *et al.*, Phys. Rev. D23, 604 (1981); P. Bordalo, *et al.*, Phys. Lett. 193B, 368 (1987).

44. Yu. M. Antipov, *et al.*, Phys. Lett. 76B, 235 (1978); M. J. Corden, *et al.*, Phys. Lett. 110B, 415 (1982); J. Badier, *et al.*, Z. Phys. C20, 101 (1983); S. Katsanevas, *et al.*, Phys. Rev. Lett. 60, 2121 (1988).

45. P. Hoyer, M. Vanttinen, and U. Sukhatme, HU–TFT–90–14, (1990.)

46. S. J. Brodsky, P. Hoyer Phys. Rev. Lett. 63, 1566 (1989).

47. Alternatively, the individual charmed quarks can fragment into final state charmed hadrons either by hadronization or by coalescing with co–moving

light quark spectators from the beam. This effect can explain the depletion of the ratio of J/ψ to continuum muon pairs in high transverse energy nucleus–nucleus collisions. See S J. Brodsky and A. H. Mueller, Phys. Lett. B206, 685 (1988).

48. S. J. Brodsky, H. E. Haber, and J. F. Gunion, in *Anti–pp Options for the Supercollider,* Division of Particles and Fields Workshop, Chicago, IL, 1984, edited by J. E. Pilcher and A. R. White (SSC–ANL Report No. 84/01/13, Argonne, IL, 1984), p. 100. S. J. Brodsky, J. C. Collins, S. D. Ellis, J. F. Gunion, and A. H. Mueller, published in Snowmass Summer Study 1984, p. 227.

49. J. Ashman *et al.*, *Phys. Lett.* 202B, 603 (1988) and CERN–EP/88–06 (1988) M. Arneodo *et al.*, *Phys. Lett.* 211B, 493 (1988)

50. R. G. Arnold *et al.Phys. Rev. Lett.* 52, 727 (1984) and SLAC–PUB–3257 (1983)

51. J. S. Bell, *Phys. Rev. Lett.* 13, 57 (1964)

52. L. Stodolsky, *Phys. Rev. Lett.* 18, 135 (1967)

53. S. J. Brodsky and J. Pumplin, *Phys. Rev.* 182, 1794 (1969)

54. J. J. Sakurai and D. Schildknecht, *Phys. Lett.* 40B, 121 (1972); *Phys. Lett.* 41B, 489 (1972); *Phys. Lett.* 42B, 216 (1972)

55. R. J. Glauber, in *Lectures in Theoretical Physics*, edited by W. E. Brittin *et al.*(Interscience, New York, 1959), vol. I

56. T. H. Bauer, R. D. Spital, D. R. Yennie and F. M. Pipkin, *Rev. Mod. Phys.* 50, 261 (1978)

57. P. V. Landshoff, J. C. Polkinghorne and R. D. Short, *Nucl. Phys.* B28, 225 (1971)

58. S. J. Brodsky, F. E. Close and J. F. Gunion, *Phys. Rev. D* 5, 1384 (1972)

59. S. J. Brodsky, and H. J. Lu, *Phys. Rev. Lett* 64, 1342 (1990)

60. A. H. Mueller and J. Qiu, *Nucl. Phys.* B268, 427 (1986)
J. Qiu, *Nucl. Phys.* B291, 746 (1987)

61. N.N. Nikolaev and V. I. Zakharov, MPI–PAE–PTh–11/90, (1990); Physics Letters 55B 397 (1975); Sov. J. Nucl. Phys. 21, 227 (1975).

62. A.H. Mueller, CU–TP–475, DESY Lectures given at the Small–x Workshop, DESY, May (1990).